Vertical Edge Detection-Based Automatic Optical Inspection of HGA Solder Jet Ball Joint Defects

Jirarat Ieamsaard[1], **Suchart Yammen**[2],
Paisarn Muneesawang[3], and **Frode Eika Sandnes**[4], Non-members

ABSTRACT

The Head Gimbal Assembly (HGA) is an essential hard disk drive (HDD) component allowing data to be read from and written to the media. Defects on the HGA may affect the data read/write process and reduce the quality of the HDD. Therefore, HGA inspection needs to be improved during HDD manufacturing. This paper describes an image processing method that automate the optical inspection of HGA solder jet ball joint defects. Vertical edge detection methods are proposed for identifying defects. The performance of the vertical edge detection method is compared to a Sobel-based method, Roberts' method and a Prewitt's method. The methods were tested with 18,123 HGA images. The experimental results show that the vertical edge detection method outperforms the other methods, which had an accuracy of 99.3%, as compared to the Sobel based method, with an accuracy of 80% and 78.2 for Roberts' method and 65.9 for Prewitt's method.

Keywords: Optical Inspection, Solder Jet Ball Joint Defect, Vertical Edge Detection

1. INTRODUCTION

The Head Gimbal Assembly (HGA) is an important part of the read/write assembly in a hard disk drive (HDD). Technological hard disk advancements have resulted in units with very small form factors. Therefore, increasing attention has been focused on the quality inspection of small components. The HGA consists of a slider and a suspension mechanism. A solder jet bond (SJB) machine is used in HGA production to attach the slider to the suspension mechanism. During this process mistakes sometimes occur causing defects. Currently, the HGAs are manually inspected. Manual inspection may lead to weariness and eye strain, especially with a large number of units. Moreover, manual inspection is time-consuming and may cause production delays, it is expensive and may reduce customer confidence. The goal is therefore to develop an automatic inspection system to reduce the chance of errors, reduce costs and improve the productivity.

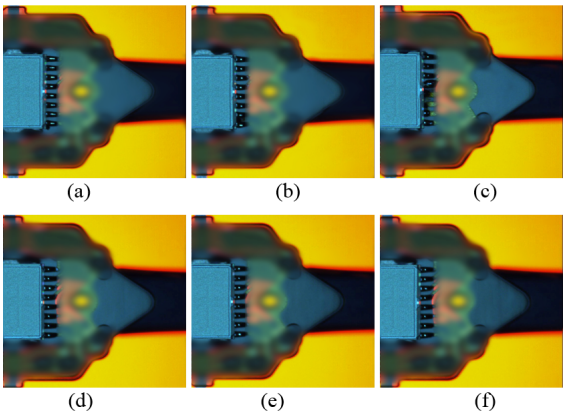

Fig.1: *Sample HGA Images; (a), (b), and (c) show non-defective HGAs, (d), (e), and (f) show defective HGAs.*

This study focused on the most significant defect that can occur in the solder joint between the slider and the HGA suspension mechanism, namely when the solder balls or pads become burnt (see Fig. 1). Characteristics of defects caused by soldering include uneven pad edges or black limbs on pad borders. Other HGA defects including solder ball bridging and incomplete solder joints on both sides of the slider and suspension have previously been studied using morphological template matching [1-2]. However, the defects caused by solder ball burning cannot be detected by morphological template matching or other methods that rely on the general shape features of the burnt area such as area size, perimeter, or center of mass.

This paper proposes a new vertical edge detection algorithm that more effectively identify HGA defects caused by burnt solders and pads.

Manuscript revised on October 18,2015.
[1,2,3] The authors are with Department of Electrical and Computer Engineering, Naresuan University, Phitsanulok, Thailand., Email:jirarati55@email.nu.ac.th, sucharty@nu.ac.th and paisarnmu@nu.ac.th
[4] The author is with Institute of information Technology, Faculty of Technology, Art and Design, Oslo and Akershus University College of Applied Sciences, Oslo, Norway., Email:Frode-Eika.Sandnes@hioa.no
[4] The author is with Westerdals Oslo School of Art, Communication and Technology, Oslo, Norway., Email:Frode-Eika.Sandnes@hioa.no

2. PREVIOUS WORK

Several experimental studies have addressed hard disk drive defects inspection including detection of defects on the HDD media surface using spectral imaging [3-4]. Kunakornvung et al. [5] detected the presence of contamination on the Air Bearing Surface (ABS) of the slider using texture characteristics. Withayachumnankul et al. [6] designed a filter kernel to detect the edge of hairline crack defects on the surface of piezoelectric actuators. Yammen et al. [7] detected corrosion on the pole tips at the end of an air-bearing slider, using area-based and contour-based features. Mak et al. [8], proposed a Bayesian approach for solder joint defects addressing solder bridging, burnt solder balls, non-wet, dry joints and cases with no connections between the slider and suspension. This paper, however, focuses on burnt solder ball defects, which is the most significant unresolved problem.

Edge detection is an essential component of many image analysis systems [9-10]. The Sobel edge detection operator is typically used for object segmentation, see for instance Zhang et al. [11] and Fan et al. [12]. The Sobel operator detects horizontal and vertical edges separately, and some application domains take advantage of this, such as license plate detection [13-14]. Prewitt and Roberts [15] are traditional edge detectors, which work by calculating the horizontal and vertical image gradients. Al-Ghaili et al. [16-17] presented a fast vertical edge detection algorithm, which concentrates on the intersections of the black-white regions and the white-black regions.

This work extend Al-Ahaili et al.'s vertical edge detection and applies the algorithm to the problem of burnt pad defection. The experimental results show that the proposed method achieves an accuracy of 99.3% with a low false detection rate of 0.% and a false negative rate of 0.2%.

3. BURNT SOLDER BALL DETECTION

This study uses edge detection and a circular Hough transform to identify burnt pad defects. In the HGA production line, the SJB machine first connects the suspension circuit to the slider body. Then, the HGAs are placed on pallets and transferred to a Visual Inspection and OCR Reading (VOR) machine. A COGNEX software module is used by the VOR for automatic vision processing. HGA images are first captured before these images are processed to detect HGA defects. The results are sent to the module controller. If the COGNEX subsystem detects faults the unit is manually inspected. The COGNEX system yield a very high false positive rate and consequently a large amount of units need the time-consuming, costly and error-prone manual intervention.

This research focuses on the defects of the solder joints between the slider and suspension. To detect burnt pad defects, the top view of HGA images is used. The top view shows the small burnt pads more clearly than other views.

3.1 Sobel-Based Method

This section presents the algorithm for solder ball and pad burning detection based on Sobel edge detection. The image processing techniques and the Sobel vertical edge detector are adopted in order to identify the defects in the input images. The overall algorithm procedure is given in Algorithm 1.

Algorithm1: Sobel-based method Input: *HGA Image*

1. Pre-Processing

Segment the ROI from the *Original HGA Image*

Make a binary *sub-image* from the blue channel intensity.

Fill holes in each pad located in the binary sub-image.

2. Vertical edge analysis

Apply Sobel to detect the vertical edges.

Remove the vertical edge of the solder tail.

Identify solder burns.

3. Make decision

If (summation of edge pixel > decision value)

Result = defect found.

Else

Result = non-defective.

End If

First, region of Interest (ROI) segmentation is performed using cross correlation [7, 18] between the original 2400 × 2000 pixel test image $f[m,n]$ and the 45 × 420 pixel template image $\{w[m,n]\}$. The template image only contains the solder joint region, and is manually extracted from a perfect HGA image chosen manually by an inspector. The cross-correlation function is obtained as

$$r_{fw}[m,n] = \sum_{s=0}^{44}\sum_{t=0}^{420} f[s,t]w[m+s,n+t] \qquad (1)$$

where, m and n are the coordinates $m \in 0,1,\ldots,2400$, $n \in 0,1,\ldots,2000$. By finding the maximum value of the cross-correlation function, the best matching image can be obtained. That is, $r_{fw}[m_0,n_0] = \max m,n\ r_{fw}[m,n]$, where the coordinate $[m_0,n_0]$ gives the maximum value. This coordinate is used to generate the output solder joint image, $\{f[m_0+m,n_0+n]\}$. The RGB color HGA image is the input image. The blue channel is chosen as basis for the binary image since it shows the difference between the solder balls and the gap region more clearly than the red and green color channels. Figs. 2 and 3 show that the blue channel histogram has a wider distribution than the red and green channels. The optimum hardness threshold is then defined and the blue channel is transformed into a binary image. The binary sub-image may contain solder balls with holes

inside their boundary. Morphological reconstruction is therefore used to fill these holes [19].

Fig.2: *Red, green, and blue intensity of a ROI image.*

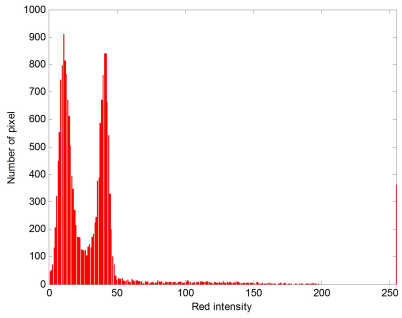

(a)

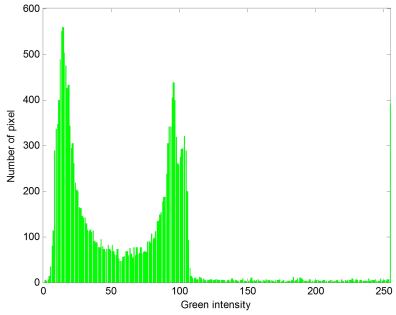

(b)

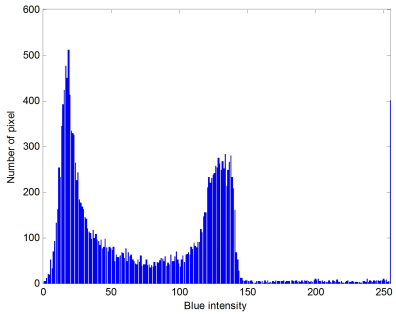

(c)

Fig.3: *Histogram of each channel (a) red channel, (b) green channel, and (c) blue channel.*

A Sobel edge detector [9-14] is used to analyze the vertical edges of the solder balls. As some of the solder tails may appear in the binary sub-image the vertical edge of the solder balls is checked and removed using a threshold value. If the size of the detected vertical edge is larger than a pre-defined threshold, the algorithm assumes that the vertical edge is the edge of the solder tail, and not the burnt area. The detected vertical edge is therefore removed. After removing the solder tail vertical edge, the binary sub-image only contains the vertical edge of the burnt solder balls, as well as the small burnt objects in the gap between the solder balls.

Finally, the algorithm decides whether the test image is defective or not. After analyzing the vertical edge, the white pixels in the binary sub-image correspond to the vertical edge of the solder balls that are burnt and some small burnt objects. To make a decision, a decision value is generated by the summation of all the pixels of the binary sub-image resulting from the previous step. If the decision value is greater than this threshold value, the test image is a defective image; otherwise, the test image is a non-defective image. Fig. 4 shows the result of each step, Fig. 4 (a) shows the result of a non-defective image, and Fig. 4 (b) shows the result of a defective image containing the solder ball or pad defect. Fig. 5 shows the result and samples of the output image. Fig. 5 (a)-(b) represent non-defective test images and Fig. 5. (c)-(d) represent defective test images. The images are rotated for presentation purposes.

(a)

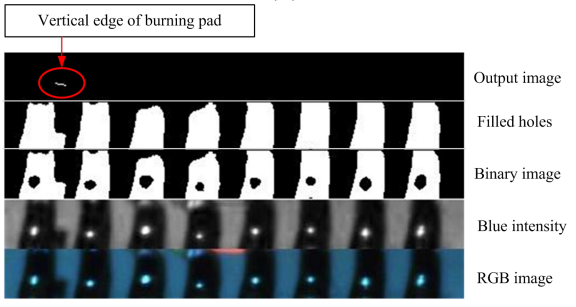

(b)

Fig.4: *Detection results obtained with Sobel-based Method, (a) non-defective example, and (b) defective example.*

False detections occurred due to the reflections that appeared on the pads. These reflections were detected as edges by the Sobel operator and resulted in incorrect decisions. The image capturing process

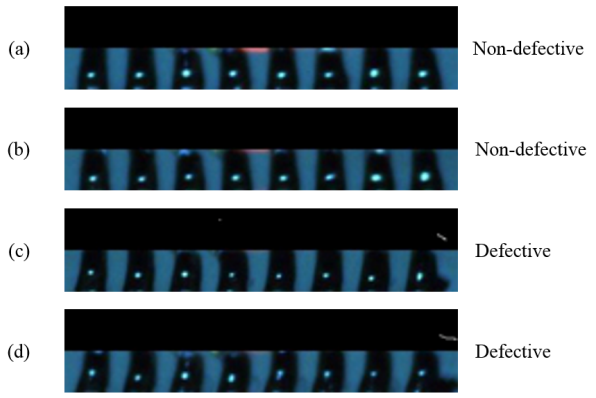

Fig.5: *Result of the Sobel-based method, (a) and (b) non-defective image, (c) and (d) defective image.*

may illuminate each local area differently, e.g. the right side may be darker than the left side. The optimum hardness threshold is unable to separate the pad from the background under such lighting conditions (see Fig. 6).

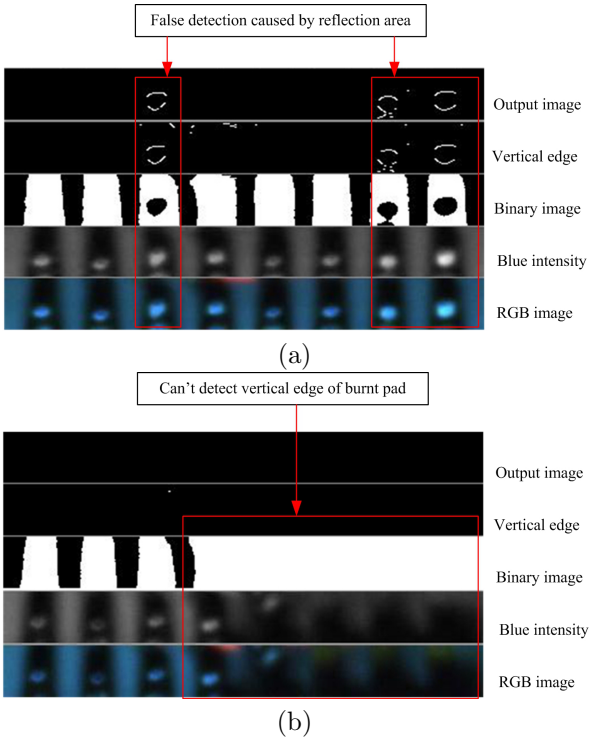

Fig.6: *False detection produced by the Sobel-based method; (a) caused by reflection, (b) caused by lighting effect.*

3.2 The Proposed Method

The reflections cause unwanted vertical edges when using the Sobel-based method which again leads to false detections. The errors caused by the unwanted vertical edges was reduced by determining the reflection area on each pad and then removing the vertical edge in each of these areas. For cases where a burn covers the entire pads and the vertical edge cannot be detected, an area-based feature is used. The procedure of the overall algorithm is shown in Fig. 7.

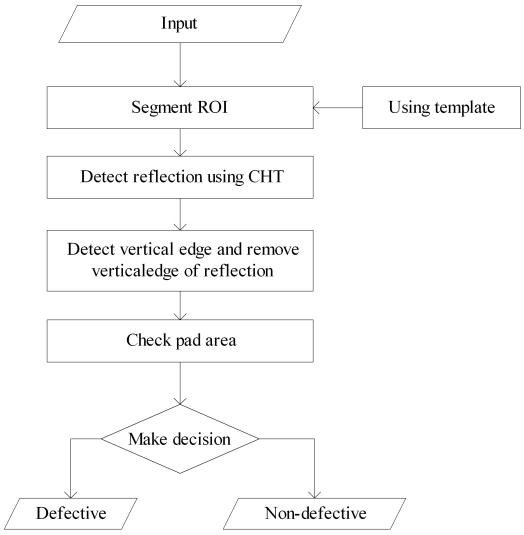

Fig.7: *The proposed method.*

The algorithm begins with an ROI segmentation; the solder joint area is the region of interest and is extracted by using cross correlation [7, 18]. The 2400 $\times$ 2000 pixel input HGA image is correlated with the 45 $\times$ 420 pixel template image. The point giving the highest correspondence between the input image and the template image is the reference point. From the reference point, the 45 $\times$ 420 pixel region of interest is extracted as a sub image.

The light reflections appears as white circular objects within the pad. To detect these reflection areas, the circular Hough transform [21] is applied, where circles are representd using:

$$r^2 = (x-a)^2 + (y-b)^2 \tag{2}$$

Here, a and b represent the coordinates for the circle center, and r denote the radius of the circle. The parametric representation of this circle is:

$$x = a + r\cos(\theta) \tag{3}$$
$$y = b + r\sin(\theta) \tag{4}$$

When the angle θ sweeps through a full 360 degrees circle, the points (x, y) trace the circle perimeter. If an image contains many points, some of which fall on the perimeters of circles, the objective is to find parameter triplets (a, b, R) to describe each circle. The locus of (a, b) points in the parameter space fall on a circle of radius R centered at (x, y). The true center point will be common to all parameter circles, and can be found with a Hough accumulation array [21]. Fig. 8 shows an example of using the circular Hough

transform for reflection detection.

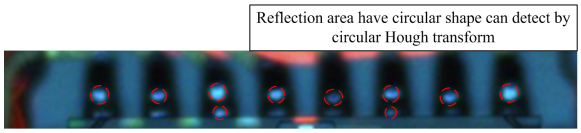

Fig.8: *Reflection Area Detection.*

Before applying vertical edge detection, the solder image is transformed into a binary sub-image using Otsu's method [20]. An optimal threshold is selected by the discriminate criterion to maximize the reparability of the resulting gray level classes. The procedure utilizes only the zeroth and the first order cumulative moments of the gray level histogram. Otsu's method exhaustively searches for the threshold that minimizes the within-class variance, defined as a weighted sum of variances,

$$\sigma^2_{within}(t) = \omega_1(t)\sigma^2_1 + \omega_2(t)\sigma^2_2(t) \qquad (5)$$

The weights ω_i are the probabilities of the two classes separated by a threshold t and variances σ^2_i of these classes. Using Otsu's method, the solder region can be separated from the background with more accuracy than by using the optimal hard threshold.

Withayachumnankul et al. [6] designed a filter kernel to detect the edges of hairline crack defects on the surface of hard disk drive piezoelectric actuators. The kernel filter can detect lines at multiple angles with a complicated computation procedure. Al-Ghaili et al. [16-17] presented a vertical edge detection algorithm (VEDA) to detect license plate numbers. Their results showed that VEDA has a high accuracy and is about nine times faster than the Sobel operator. VEDA [16-17] was therefore adapted in this study. The VEDA focuses on pixel transitions from black to white and from white to black, by moving a 2x4 mask (shown in Fig. 9) from left to right and from right to left, as described in Algorithm 2.

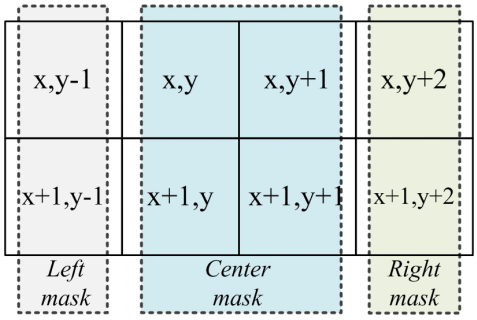

Fig.9: *A 2×4 Window Mask.*

Algorithm 2: VEDA

Input: *Binary Image*
Create a white blank image as *Image(x,y);*

For every pixel in the *Binary Image*
center=1; left=1; right=1;
If (all center mask values = black)
center=0;
End If
If (all right mask values = black)
right=0; **End If**
If (all left mask values = black)
left=0; **End If**
If *(!center AND !right AND !left)*
Image(x,y)=white;
Image(x,y+1)=black;
End If
End For

Through this process, the black-white and white-black regions are located. Using this 24 window mask, a one- and two-pixel thick edge is detected for each pad. VEDA is about nine times faster than Sobel [16-17]. The time-complexity of VEDA is O(NM) and the time-complexity of vertical Sobel is O(N×M×K). where N and M represent the iterations in the first and the second loop inside the Sobel and the VEDA codes and K is the number of iterations of the third loop, namely the size of vertical Sobel mask scale. The Prewitt edge detector time-complexity is equal to the time-complexity of Sobel because it use a vertical mask with the same size as Sobel. Next, the Roberts vertical edge detector has the same time-complexity of O(N×M×K), but K is smaller since the vertical edge mask is smaller in the Roberts method than in the Sobel and Prewitt methods. In conclusion, the time- complexity of VEDA is smaller than that of Roberts, Sobel, and Prewitt methods.

Fig. 10 shows example results of the reflection area detection and VEDA output images for both defective- and non-defective images. Images are rotated for presentation purposed. Fig. 10 (a) shows a non-defective exemplar and Fig. 10 (b) shows a defective exemplar.

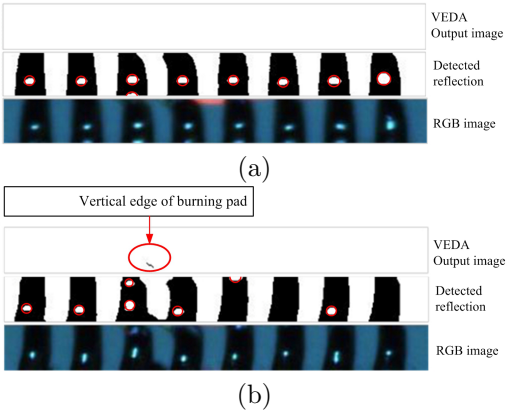

Fig.10: *Reflection area detection and VEDA output image, (a) non-defected image, and (b) defected image.*

In order to improve the decision process, the vertical reflection edge within the pad is removed by checking for black pixels. If a black pixel occur within the area of reflection, that black pixel is set to white (background color). Namely,

$$\mathrm{I(x,y)} = \begin{cases} 255 & if\ (x,y)\ is\ in\ the\ reflection\ area \\ I(x,y), & otherwise \end{cases}. \quad (6)$$

In [7] an area-based feature was used to identify corrosion on the pole tip on the actuator component of HGAs. In this study, a similar area-based feature is used to identify burnt pads whose burnt area covers the entire pad from bottom to top, thereby having no vertical edges. The area of 168 non-defective pads and 34 burnt pads were collected. Maximum and minimum areas of non-defective pads were 70% and 44% of pad ROI, respectively. For defective samples, both small burnt pads and large burnt pads were collected. Maximum and minimum areas of burnt pads were 93% and 19% of pad ROI, respectively. Fig. 11 shows samples of non-defective pads (a) and burnt pads (b) annotated with the percentage pad area.

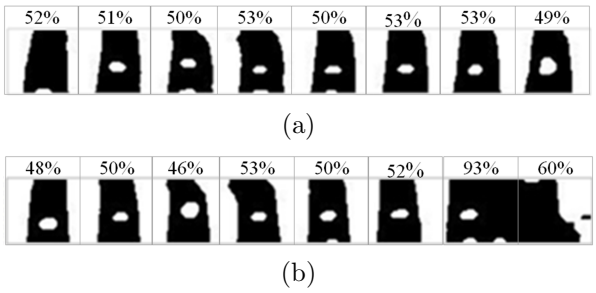

Fig.11: *Example pad areas (a) non-defective pads, and (b) burnt pads (two pads to the right).*

From the maximum area of non-defective pads a threshold T was obtained as shown in (7). If the pad area is greater than the threshold T, the pad is defective. The threshold for a pad area is obtained using:

$$T = \left(\frac{Area\ of\ ROI}{Number\ of\ pads} \right) \times Max\ Pad\ Area \quad (7)$$

Finally, the algorithm decides whether the HGA is defective. In the vertical edge image, the black pixels in the binary sub-image that correspond to the vertical edge of the burnt solder balls, and some small burn traces. To make a decision, a vertical edge value is generated by counting the black pixels of the pad image resulting from the previous step. If the vertical edge value is greater than a vertical edge threshold or the pad area is greater than the pad's threshold, the test image shows a defective HGA; otherwise, the test image shows a non-defective HGA. Detection result of the purposed method is shown in Fig. 12. The results and output image of the proposed method are shown in Fig. 13, where Fig. 13 (a)- and (b) refer to non-defective exemplars and Fig. 13 (c) and (d) refer to defective exemplars.

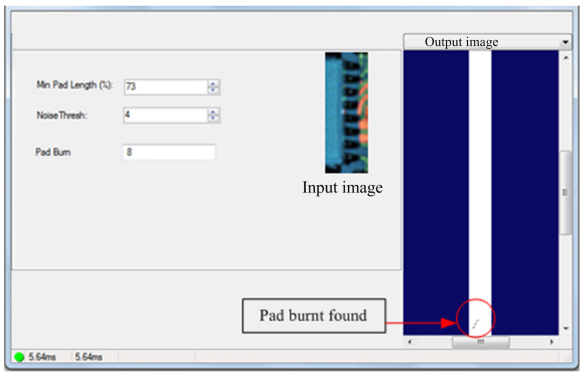

Fig.12: *Burnt solder ball detection with the proposed method.*

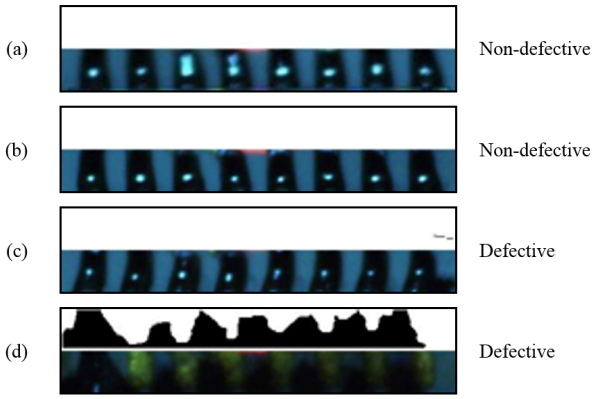

Fig.13: *Result of the Proposed Method, (a) and (b) non-defective image, (b)-(c) defective image.*

However, there are a few false detections caused by the large area and unusual shape caused by reflections (see Fig. 14 (a)) and some false detections are caused by small traces of burns of the last pad (see Fig. 14 (b)).

4. EXPERIMENTAL RESULTS

For the experiment 18,123 HGA images comprising 17,564 non-defective HGAs and 559 defective HGAs were acquired by a mechanical positioning tool. The mechanical positioning tool holds the camera in a fixed position and takes the pictures. Although the camera is in a fixed position resulting in the same size and resolution the mechanical positioning tool is unable to control the lighting condition. The 2400×2000 pixel RGB images used in this experiment had a resolution of 96 dpi. The HGA images were collected from production line during an extensive time period and from various HGA images.

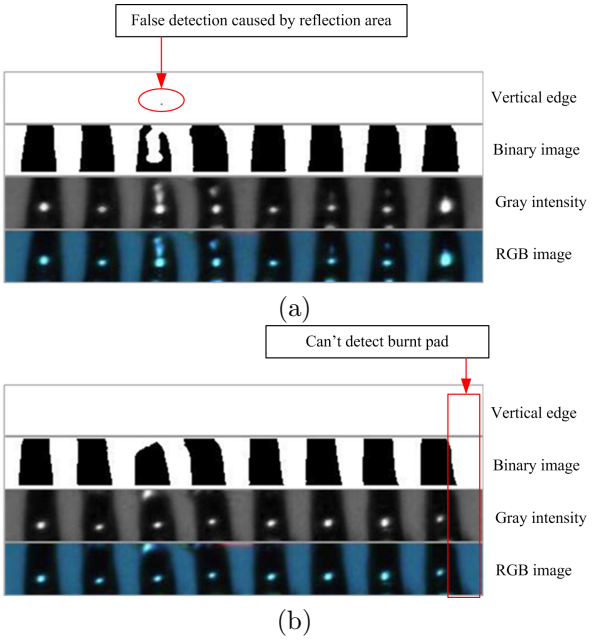

Fig.14: *False detections caused by (a) reflection, (b) small burn traces.*

Pads were classified as burnt if at least one of its edges was uneven or its border had a black limb. Experiments were conducted to evaluate the performance of the proposed method compared with the Sobel-based, Prewitt-based and Roberts-based methods. The methods were implemented in Matlab and run on a Windows laptop with Core i5 CPUs 2.5 GHz, and 4 GB of RAM. The proposed method takes 0.71 seconds per image which is shorter than the Sobel-based method taking 0.97 seconds per image and the Prewitt-based method taking 0.92 seconds per image. The computation time of the proposed method is longer than the Roberts-based method (0.64 seconds per image). This is due to the nature of the implementation. Our results thus confirm that vertical VEDA is faster than vertical Sobel. The computation time of each step shown in Table 1.

Table 1: *Computation time measured using "profile on/viewer" in MATLAB.*

	Computation time for each step						Total computation time (s)
	Segment ROI	Detect reflection	VEDA	Remove unwanted edge	Check area	Make decision	
Proposed method	0.32	0.22	**0.05**	0.05	0.02	0.05	**0.71**
	Segment ROI	Detect reflection	VEDA	Remove unwanted edge		Make decision	
Sobel	0.32	0.19	**0.37**	0.05		0.04	**0.97**
Prewitt	0.32	0.19	**0.32**	0.05		0.04	**0.92**
Roberts	0.32	0.19	**0.04**	0.05		0.04	**0.64**

False detection is a key issue in the HDD industry, and methods are therefore compared using false positive- and false negative rates. Comparisons are also made to the popular Prewitt and Roberts vertical edge detection algorithms. The proposed method yields the lowest false positive- and false negative rates of 0.7% and 0.2%, respectively. The Sobel-based method yields 20.4% false positive- and 5.4% false negative rates, The Prewitt-based method yields 21.6% false positive- and 30.6% false negative rates, while the Roberts-based method gives 34.6% false positives and 18.8% false negatives. The experimental results are listed in Table 2.

Table 2: *Detection results.*

	Sobel		Prewitt		Roberts		Our method	
Non-defective (17,564 images)		%		%		%		%
True positive	13,973	79.6	13,776	78.4	11,493	65.4	17,442	99.3
False positive	3,591	20.4	3,788	21.6	6,071	34.6	122	0.7
Defective (559 images)								
True positive	529	94.6	388	16.9	454	81.2	558	99.8
False positive	30	5.4	171	30.6	105	18.8	1	0.2

Four performance evaluation measurements were used [22]; sensitivity, specificity, precision, and accuracy (see Table 3). The proposed method achieved 99.3% accuracy while the Sobel, Prewitt, and Roberts-based methods achieved 80.0%, 78.2% and 65.9%, respectively. The proposed method provided a high specificity and precision of 99.8% and 99.9%, while the Sobel-based method achieved a specificity of 94.6% and precision of 99.8%, the Prewitt-based method achieved a specificity of 69.4% and a precision of 99.8%, and the Roberts-based method achieved a specificity of 81.2% and precision of 99.1%. For the sensitivity, which is of prime concern in the HDD industry, the proposed vertical edge detection method achieved a sensitivity of 99.31% while the Sobel-based method achieved a sensitivity of 79.5%, the Prewitt-based method and the Roberts-based method achieved sensitivities of 78.4% and 65.4%, respectively.

Table 3: *Performance Evaluation.*

Method	Sensitivity	Specificity	Precision	Accuracy
Sobel-based method	79.5	94.6	99.8	80.0
Prewitt-based method	78.4	69.4	99.8	78.2
Roberts-based method	65.4	81.2	99.1	65.9
Our method	99.3	99.8	99.9	99.3

5. LIMATIONS

Tests were performed using low resolution images, while a resolution may be higher in a production setting. The resolution of the HGA images should be sufficiently high to clearly see the burnt defect. Small burnt defects might not be detected if the image is blurred. The proposed method might be applied to detect other types of solder ball defects, such bridging between two solder balls, incomplete solder balls on both sides of the slider and suspension, and missing solder balls on the pads.

6. CONCLUSION

A vertical edge detection method for the detection of defects in solder joints of HGA in case of solder balls or pads burning was proposed. The method adopt the circular Hough transform to detect reflections that occur during the image capturing process. Cases where the burning area covered the entire pad was detected using an area-based feature. The performance of the proposed method was compared with those of the Sobel, Prewitt and Roberts-based methods. Experimental results validated the effectiveness of the proposed method over the Sobel, Prewitt and Roberts-based methods in term of accuracy, sensitivity, specificity, precision and false detection rate.

ACKNOWLEDGMENT

This project is financially supported by the Thailand Research Fund (TRF).

References

[1] P. Muneesawang, S. Yammen, T. Fuangpian, and J. Ieamsaard, "Morphology-based Automatic Visual Inspection for SJB Defect on HGA," *Proceeding of 4^{th} International Data Storage Technology Conferenc. (DST-CON)*, pp. 32-35, 2012.

[2] J. Ieamsaard, B. Tangdee, S. Yammen, P. Muneesawang, "Solder Joint and Styrofoam Bead Detection in HDD Using Mathematical Morphology," *Proceeding of International Computer Science and Engineering Conference (ICSEC 2012)*, pp. 99-104, 2012.

[3] Z. S. Chow, M. Po-Leen Ooi, Y. C. Kuang, S. Demidenko, "Low-cost Automatic Visual Inspection System for Media in Hard Disk Drive Mass Production," *Proceeding of Instrumentation and Measurement Technol Confefence (I2MTC)*, pp. 234-239, 2012.

[4] Z. S. Chow, M. Po-Leen Ooi, Y. C. Kuang, S. Demidenko, "Automated Visual Inspection System for Mass Production of Hard Disk Drive Media," *Elsevier, Procedia Engineering*, vol 41, pp. 450-457, 2012.

[5] P. Kunakornvong, C. Tangkongkiet, and P. Sooraksa, "Defect Detection on Air Bearing Surface with Luminance Intensity Invariance," *Proceeding of 9^{th} International Conference on Fuzzy Systems and Knowledge Discovery (FSKD)*, pp. 693 - 696, 2012.

[6] W. Withayachumnankul, P. Kunakornvong, C. Asavathongkul, and P. Sooraksa, "Rapid Detection of Hairline Cracks on the Surface of Piezoelectric Ceramics," *The International Journal of Advanced Manufacturing Technology*, vol. 64, Issue: 9-12, pp.1275-1283, 2013.

[7] S. Yammen, and P. Muneesawang, "An Advanced Vision System for the Automatic Inspection of Corrosions on Pole Tips in Hard Disk Drives," *IEEE Transactions on Components, Packaging, and Manufacturing Technology*,vol.4, Issue:9, pp. 1523-1533, 2014.

[8] C. W. Mak, N. V. Afzulpurkar, M. N. Dailey, and P. B. Saram, "A Bayesian Approach to Automated Optical Inspection for Solder Jet Ball Joint Defects in the Head Gimbal Assembly Process," *IEEE Transaction on Automation Science and Engineering*, vol. 11, Issue:4, pp. 1155-1162, 2014.

[9] K. Shah, K. Patel, and G. I. Prajapati, "Various Edge Detection Techniques: Survey, Implementation and Comparison," *International Journal of Advanced Research in Computer Science*, vol. 4, no. 4, pp. 109-113, 2013.

[10] D. R. Waghule, and R. H. Ochawar, "Overview on Edge Detection Methods," *Proceeding of Electronic Systems, Signal Processing and Computing Technologies (ICESC)*, pp. 151-155, 2014.

[11] H. Zhang, Q. Zhu, and X. Guan, "Probe into Image Segmentation Based on Sobel Operator and Maximum Entropy Algorithm," *Proceeding of International Conference on Computer Science & Service System (CSSS)*, pp. 238-241, 2012.

[12] Y. Fan, B. Lin, and S. Chou, "Hardware Structure of 2D to 3D image Conversion System for Digital Archives," *Proceeding of 17^{th} International Symposium on Consumer Electronics (ISCE)*, pp. 111-112, 2013.

[13] Y. Qiu, M. Sun, and W. Zhou, "License Plate Extraction Based on Vertical Edge Detection and Mathematical Morphology," *Proceeding of International Conference on Computational Intelligence and Software Engineering (CiSE)*, pp. 1-5, 2009.

[14] L. Li, Y. Han, and H. Hahn, "License Plate Detection Method Using Vertical Boundary Pairs and Geometric Relationships," *Proceeding of International Conference on Computer Engineering and Technology (ICCET)*, pp. V2-581 - V2-585, 2010.

[15] Kumar, Tapas, and G. Sahoo. "A novel method of edge detection using cellular automata," *International Journal of Computer Applications*, vol 9, no. 4, pp 38-44, 2010.

[16] A. M. Al-Ghaili, S. Mashohor, A. R. Ramli, and A. Ismail, "Vertical-Edge-Based Car-License-Plate Detection Method," *IEEE Transactions on Vehicular Technology*, vol. 62, Issue: 1, pp. 26-38, 2013.

[17] A. M. Al-Ghaili, S. Mashohor, A. Ismail, and A. R. Ramli, "A New Vertical Edge Detection Algorithm and Its Application," *Proceeding of International Conference on Computer Engineering & Systems (ICCES)*, pp. 204-209, 2008.

[18] P. Liang, X. Zhiwei, and D. Jiguang, "Fast Normalized Cross-correlation Image Matching

Based on Multiscale Edge Information," *Proceeding of International Conference on Computer Application and System Modeling (ICCASM)*, pp. 507-511, 2010.

[19] M. S. Mohammad, and A. Mahloojifar. "Retinal image analysis using curvelet transform and multistructure elements morphology by reconstruction," *IEEE Transactions on Biomedical Engineering*, vol. 58, Issue: 5, pp. 1183-1192, 2010.

[20] N. Otsu, "A Threshold Selection Method from Gray-level Histograms," *IEEE Transaction on Systems, Man and Cybernetics*, vol. 9, no. 1, pp. 62-66, 1979.

[21] C. Chang, T. Chao, J. Horng, C. Lu, and R. Yeh, "Development pattern recognition model for the classification of circuit probe wafer maps on semiconductors," *IEEE Transactionon on Components, Packaging and Manufacturing Technology*, vol. 2, Issue: 12, pp. 2089 -2097, 2012.

[22] J. Han and M. Kamber, *Data Mining: Concepts and Techniques*, San Francisco, CA, USA: Morgan Kaufmann, 2006, ch. 6.

Jirarat Ieamsaard received the B.Eng. (Computer Engineering) and M.Eng. (Electrical Engineering) from Naresuan University, Phitsanulok, Thailand, in 2008 and 2011, respectively. She is currently pursuing a Ph.D. degree at Naresuan University, Phitsanulok, Thailand. Her current research interests include image processing, machine learning, and automatic visual inspection.

Suchart Yammen received the bachelor's (Hons.) degree in electrical engineering from Chiang Mai University, Chiang Mai, Thailand, in 1988, and the M.S. and Ph.D. degrees from Vanderbilt University, Nashville, TN, USA, in 1998 and 2001, respectively. He was a Supervisor with the Colgate-Palmolive (Thailand) Company, Ltd., Bangkok, Thailand, in 1988, and served in the powder plant. From 1989 to 1993, he was with Siam Cement Public Company, Ltd, Bangkok, as a Production Engineer, a Maintenance Engineer, and a Project Engineer. In 1994, he joined Naresuan University, Phitsanulok, Thailand, where he is currently an Assistant Professor of Electrical Engineering. He has coauthored of *Visual Inspection Technology in the Hard Disk Drive Industry* (London, UK: Wiley-ISTE, 2015), *The Era of Interactive Media* (New York, NY, USA: Springer Publisher, 2012) and *Principles of Communications* (Bangkok, Thailand: Chulalongkorn University Press, 2011). His current research interests include renewable energy, communication and control theory, signal processing, system identification, and modeling. Dr. Yammen is a Senior Member of the Institute of Electrical and Electronics Engineers (IEEE), a member of Council of Engineers and a Fellow Member of the Engineering Institute of Thailand.

Paisarn Muneesawang received the B.Eng. degree in electrical engineering from the Mahanakorn University of Technology, Bangkok, Thailand, in 1996, the M.Eng.Sci. degree in electrical engineering from the University of New South Wales, Sydney, NSW, Australia, in 1999, and the Ph.D. degree from the School of Electrical and Information Engineering, University of Sydney, Sydney. He was a Post-Doctoral Research Fellow with Ryerson University, Toronto, ON, Canada, from 2003 to 2004, and an Assistant Professor with the College of Information Technology, University of United Arab Emirates, Al Ain, United Arab Emirates, from 2005 to 2006. He has held Visiting Professorships with the Nanyang Technological University, Singapore, and Ryerson University, Toronto, ON M5B 2K3, Canada, since 2012 and 2013, respectively. He was the Vice President of Administrative Affairs, Naresuan University, Phitsanulok, Thailand, where he is currently an Associate Professor. His current research interests include multimedia signal processing, computer vision, and machine learning. He has served as the Registration Co-Chair of the International conference on multimedia and expo 2006 and the Technical Program Co-Chair of the Pacific-Rim Conference on Multimedia 2009. He has co-authored two books, *Multimedia Database Retrieval: A Human-Centered Approach* (New York, NY, USA: Springer, 2006), and *Unsupervised Learning-A Dynamic Approach* (New York, NY, USA: Wiley-IEEE Press, 2013). He is a Co-Editor of the book, *Advances in Multimedia Information Processing - PCM 2009* (New York, NY, USA: Springer, 2009). Dr. Muneesawang is a Senior Member of the Institute of Electrical and Electronics Engineers (IEEE).

Frode Eika Sandnes received a B.Sc. in computer science from the University of Newcastle upon Tyne, U.K., and a Ph.D. in computer science from the University of Reading, U.K. He is a professor in the Institute of Computer Science, Faculty of Technology, Art and Design and an adjunct professor at Westerdals Oslo School of Art, Communication and Technology. He has served one term as pro-rector for Research and internationalization at Oslo and Akershus University College of Applied Sciences. His research interests include human computer interaction, image analysis and pattern recognition. Dr. Sandnes has been instrumental in the establishment of the first master specialization in Norway that addresses universally designed computer systems. He is an editorial member of several international journals, has organized several international including UIC and ATC 2008 with proceedings on Springer LNCS and he was involved in the translation of W3Cs WCAG2.0 into Norwegian.